



CDK4/6i enhances the antitumor effect of PD1 antibody by promoting TLS formation in ovarian cancer

Wangyou Feng^a, Dongbo Jiang^b, Ying Xu^a, Yuanfeng Li^a, Lin Chen^a, Minye Zhao^a, Yujie Shen^a, Wenjing Liao^a, Hong Yang^{a,**}, Jia Li^{a,*}

^a Department of Gynaecology and Obstetrics, Xijing Hospital, Air Force Medical University (the Fourth Military Medical University), 15 Changle Western Road, Xi'an, 710032, Shaanxi, China

^b Department of Immunology, School of Basic Medicine, Air Force Medical University (the Fourth Military Medical University), 169 Changle Western Road, Xi'an, 710032, Shaanxi, China

ARTICLE INFO

Keywords:

CDK4/6i
TLS
PD1 antibody
Immunotherapy
And prognosis

ABSTRACT

Ovarian cancer is insensitive to immunotherapy and has a high mortality rate. CDK4/6 inhibitors (CDK4/6i) regulate the tumor microenvironment and play an antitumor role. Our previous research demonstrated that lymphocyte aggregation (tertiary lymphoid structures, TLSs) was observed after CDK4/6i treatment. This may explain the synergistic action of CDK4/6i with the anti-PD1 antibody. However, the key mechanism by which CDK4/6i promotes TLS formation has not been elucidated. We examine the link between TLS and prognosis. Animal models and high-throughput sequencing were used to explore the potential mechanism by which CDK4/6i promotes TLS formation. Our results showed the presence of TLSs was associated with a favorable prognosis for ovarian cancer. CDK4/6i promoted TLS formation and enhanced the immunotherapeutic effect of the anti-PD1 antibody. The potential mechanism of CDK4/6i affecting the formation of TLS may be through modulating SCD1 and its regulatory molecules ATF3 and CCL4. Our findings provide a theoretical basis for the application of CDK4/6i in ovarian cancer.

1. Introduction

A prevalent malignant tumor with a high death rate in the female reproductive system, ovarian cancer poses a severe threat to the life and health of women. The recurrence rate of ovarian cancer patients is high, leading to poor prognosis [1]. At present, the treatment of PD-1/PD-L1 antibodies has become a very powerful treatment strategy, and in advanced solid tumors, an unprecedented clinical response has been shown [2]. However, PD-1 drug trials in ovarian cancer have lagged behind those in malignant melanoma and non-small cell lung cancer [3]. As early as 2007, Hamanishi J found that PD-L1 expression and the invasion degree of killer T cells in tumors are independent prognostic factors for ovarian cancer [4], which suggested that PD-1 antibodies have a good application basis in ovarian cancer. However, a phase II clinical trial using Navo antibody to treat platinum-resistant ovarian cancer showed that the total effective rate of PD-1 antibody in ovarian cancer was only 15%, and some ovarian cancer patients were insensitive to PD-1 antibody treatment or had secondary drug resistance [3]. Some small molecule inhibitors have the ability to directly modify the

* Corresponding author.

** Corresponding author. Department of Gynaecology and Obstetrics, Xijing Hospital, Air Force Medical University (the Fourth Military Medical University), 15 Changle Western Road, Xi'an, 710032, Shaanxi, China.

E-mail addresses: yanghongdoc@163.com (H. Yang), lijia219@yeah.net (J. Li).

<https://doi.org/10.1016/j.heliyon.2023.e19760>

Received 28 March 2023; Received in revised form 17 August 2023; Accepted 31 August 2023

Available online 14 September 2023

2405-8440/© 2023 The Authors. Published by Elsevier Ltd. This is an open access article under the CC BY-NC-ND license (<http://creativecommons.org/licenses/by-nc-nd/4.0/>).

immunological microenvironment of tumor tissue and encourage immune-mediated tumor eradication. For instance, BRAF inhibitors combined with anti-PD-1 or anti-PD-L1 antibodies increase melanoma patients' chances of surviving [5]. Therefore, the combination of small molecule inhibitors and immune checkpoint inhibitors (ICBs) is expected to be a new strategy for tumor therapy. Most cells express CDK4/6, a type of serine (Ser)/threonine (Thr) kinase that is an essential cell cycle regulator. Studies have demonstrated that CDK4/6 inhibitors can arrest the cell cycle in the G1 phase by specifically inhibiting CDK4/6, restoring cell cycle control, and suppressing the malignant proliferation of tumor cells. More importantly, the inhibitor can trigger the body's antitumor immunity, induce a large increase in abnormal proteins on the surface of tumor cells, and make them immune signals, which can be recognized and cleared. The main manifestations included that CDK4/6i can inhibit regulatory T cell proliferation, increase the level of T cell infiltration in tumor tissues, encourage T cell activation, and initiate effective immune responses [6–8]. This showed that CDK4/6 inhibitors enhance the immune system's attack ability and may be regulators of the immune microenvironment. Researchers have reported that the tumor-suppressing impact can be enhanced by combining CDK4/6i and PD-1 antibodies. PD-L1 protein stability and CDK4/6 activity may be related [9]. These findings support the potential of CDK4/6i to enhance anti-PD-1/PD-L1 treatment responsiveness. PD-L1 expression changed during the cell cycle and when CDK4 was reduced or inhibited. Despite RB expression, CDK4 boosted PD-L1 expression in breast cancer cells. The results from *in vivo* breast and colorectal cancer preclinical models demonstrated that CDK4/6i increased tumor susceptibility to PD-1/PD-L1 antibodies [8,9]. These results provide a rationale for increasing CDK4/6is to improve the response to anti-PD-1/PD-L1 therapy. All these findings suggest that the combination of CDK4/6is and anti-PD-1/PD-L1 antibodies may become a new treatment model for malignant tumors. Palbociclib, ribociclib, and abemaciclib are the three CDK4/6 inhibitors that have received approval to work with endocrine therapies to treat breast cancer medically with minimal adverse reactions [10,11]. However, there are also a few reports of ovarian cancer. Studies have found that abnormal activation of CDK4/6 exists in both ovarian cancer tissues and cells, and CDK4/6i can also play a certain therapeutic role in ovarian cancer mice and patients [12,13]. Only a small number of *in vivo* studies have demonstrated that CDK4/6 inhibitors decrease ovarian cancer progression, despite some *in vitro* studies demonstrating an inhibition of ovarian cancer cell proliferation [14,15]. Therefore, we previously studied the effect of CDK4/6i combined with PD1 antibody in the treatment of mouse ovarian cancer. This was the first study to prove that CDK4/6i combined with an anti-PD-1 antibody could synergistically inhibit the tumor growth of mouse ovarian cancer. Meanwhile, we observed that CDK4/6i promotes TLS formation, and thus, we suspected that this improves the immune microenvironment in ovarian cancer, which enhances the effect of PD1 antibodies [16].

A positive prognosis is linked to the presence of tertiary lymphoid structures, according to an increasing number of studies. In the same period in 2020, three articles published in *Nature* showed that the presence of TLSs in human tumors was associated with a good immunotherapy response [17–19]. The TLS is a nascent immune structure that appears in the microenvironment of inflammation, infection, or tumors, which is similar to the secondary lymphoid tissue structure and has the ability to initiate the immune response. TLSs mainly consist of T cell regions and germinal center (GC) regions. The T cell region mainly consists of T cells and mature dendritic cells (DCs). Follicular dendritic cells (FDCs), proliferating B cells, and high endothelial venules (HEVs) make up the majority of the GC area [20]. The enhancement of the tumor immune milieu will be facilitated by the synergistic interaction of T and B cells, resulting in a more effective antitumor effect and good prognosis. B cells in TLSs can cooperate with other immune cells to enhance the effect of immunotherapy by changing the activity and function of T cells [18]. However, the specific mechanisms of these effects are still under further study. Therefore, the analysis and evaluation of the dynamic changes in immune cell populations in TLSs in tumors can provide beneficial help for immunotherapy strategies. TLSs can also make antigen-presenting cells and antigen-specific T cells secrete a large number of specific chemokines, chemotactic T cells, and antigen-presenting cells so that the body can quickly produce a large number of CTLs to play an antitumor role. The existence of TLSs is highly dependent on the expression of chemokines such as CCL19, CCL21, and CXCL13 [21]. If the production of these chemokines and cytokines associated with TLS formation can be induced and stimulated, TLSs can be formed around the tumor, resulting in more immune cell infiltration. Moreover, studies have found that the presence of TLSs can enhance the immune efficacy of PD1 antibodies [18,22]. In a prior investigation, we discovered that CDK4/6i could promote the development of TLSs in mouse ovarian cancer [16]. Nevertheless, the mechanism is still unknown. Consequently, in our research, we examined how TLSs affect the prognosis of ovarian cancer patients and explored the potential mechanism by which CDK4/6i influences TLSs using animal models and high-throughput sequencing.

2. Materials and methods

2.1. Patients

Epithelial ovarian cancer patients from the Department of Obstetrics and Gynecology of Xijing Hospital before 2020 were selected. The patients were undergoing primary surgery, did not receive neoadjuvant therapy, and had no complications of other serious diseases. In addition, the patient must have complete pathological data and follow-up results. Patient case information was collected, including age, stage, lymph node metastasis, and vascular cancer thrombus. Corresponding pathological HE-stained sections of ovarian cancer tissues were obtained from the Department of Pathology of Xijing Hospital. The prognostic information of the patients was obtained by telephone follow-up. Finally, a total of 196 patients' pathological data and TLS-related information were obtained. The study protocol was approved by Medical Ethics Committee of the First Affiliated Hospital of the Air Force Medical University, and informed consent was obtained from all patients (KY20213037-1).

2.2. Animals and tumor-bearing mouse models

Female C57BL/6 mice that were six weeks old were purchased and reared at the Airforce Military Medical University's animal center in accordance with the regulations for animal experimentation. Ten percent fetal bovine serum (FBS; Gibco) and 1% penicillin-streptomycin were added to high-glucose Dulbecco's modified Eagle's medium (DMEM; Gibco) to sustain the murine ovarian cancer cell line (ID8), which was purchased from Merck Millipore (item SCC145).

To establish an animal model that can simulate human ovarian cancer, luciferase-tagged ID8 (ID8-luc) cells were intraperitoneally injected into female C57BL/6 mice that were 6 weeks old. Thirty days after tumor implantation was completed, after confirming tumor formation using the In Vivo Imaging System (IVIS; Caliper Life Science, Hopkinton, MA), the mice were randomly assigned to different groups. IVIS was used to detect tumor growth in mice. The Air Force Medical University's Laboratory Animal Welfare and Ethics Committee gave its approval to all animal research (IACUC-20230010).

2.3. Inhibitors and antibodies

Abemaciclib, a selective CDK4/6i, was purchased from MCE (New Jersey, NJ, USA). The supplier of an in vivo anti-mouse PD-1 antibody (clone RMP1-14) was purchased from BioXCell (West Lebanon, NH, USA).

2.4. Immunofluorescence (IF) and immunohistochemistry (IHC)

On paraffin slices from tumor tissues from mice and humans, IF and IHC were performed. Primary antibodies included rabbit anti-mouse CD20 (1:300, Servicebio, GB14030), rabbit anti-mouse CD4 (1:200, Servicebio, GB14064), goat anti-rat SCD1 (1:200, Affinity, DF13253), and goat anti-rat CD8 α (Bioss, 1:400, bs-10699R). DAPI (BOSTER, AR1177) was added to counterstain the nuclei. Finally, the Panoramic DESK scanning microscope system was used to capture images. Immunohistochemical images were double-blind reviewed by two pathologists with unknown tumor grade. Each case involved the collection of five randomly chosen visual fields under the microscope, and semiquantitative data were used to rate the staining intensity and the proportion of microscopy-positive cells. On the cell membrane and/or cytoplasm, the target protein was positively expressed as brownish yellow particles. The criteria for determining the staining grade of cytoplasmic stained antibodies were as follows: 1. The percentage of colored cells in cell count <5% was 0 points, 5%–25% was 1 point, 26%–50% was 2 points, 51%–75% was 3 points, and >75% was 4 points; 2. No staining was 0 points, light yellow staining intensity was 1 point, brown yellow staining intensity was 2 points, brown staining intensity was 3 points; 3. The positive grade was multiplied by the two scores: 0 is negative (–), 1–4 is weakly positive (+), 5–8 is positive (++), and 9–12 is strongly positive (+++).

2.5. Quantitative real-time PCR

Following the manufacturer's instructions, total RNA was extracted using the M5 Universal RNA Mini Kit (Mei5bio, Beijing, China) and dissolved in 30 μ L diethylpyrocarbonate (DEPC)-H₂O. Using the M5 Super plus qPCR RT kit with gDNA remover (Mei5bio, Beijing, China), total RNA was reverse-transcribed to cDNA. Relative expression levels of SCD1, ATF3, and CCL4 were quantified using 2X M5 HiPer Real-time PCR Super mix (SYBR Green, with anti-Taq). Table s1 contains a list of all primer sequences (Tsingke Biotech, Shanghai, China). The following conditions were used for the PCR cycle: initial denaturation at 95 °C for 2 min; 40 cycles of denaturation at 95 °C for 15 s, annealing at 60 °C for 15 s, and extension at 72 °C for 45 s; cooling at 35 °C for 30 s; and one cycle of melting at 60 °C for 15 s and 98 °C for 15 s. The $2^{-\Delta\Delta Ct}$ method was used to calculate relative gene expression levels after normalization to glyceraldehyde 3-phosphate dehydrogenase (GAPDH) based on reverse transcription qRT-PCR.

2.6. ELISA

Enzyme-linked immunosorbent assay (ELISA) was utilized to detect the secretion of CXCL13 (Chondrex, 6729), CCL21 (NeoBioscience, EMC127.96) and VEGFC (Novus, NBP2-78893) in the serum of mice. All operation steps and data analysis of ELISA experiments were carried out in accordance with the corresponding instructions.

2.7. High-throughput sequencing and data analysis

The prepared DNA fragments were sequenced with at least 2 replicates per group. The exon per million fragment mapping (FPKM) approach was used to quantify the levels of gene expression [23]. By using the NOISeq approach, differentially expressed genes (DEGs) were identified [24]. All DEGs were mapped to the Gene ontology (GO) database for functional classification.

2.8. Western blot analysis

Protein extractions from tumor tissue were separated using 10% or 15% SDS/PAGE before being applied to nitrocellulose membranes (BioRad, CA, USA). After blocking the membranes with 5% bovine serum albumin, the primary antibodies against SCD1 (1:2000, Affinity, DF13253), ATF3 (1:2000, Signalway Antibody, #53615), CCL4 (1:2000, Affinity, DF6545), and β -actin (1:10000, Abmart, T40104) were incubated at 4 °C overnight. In agreement with the primary antibodies, secondary antibodies were added and

incubated for 1 h at room temperature. Protein bands were detected using an Electrochemiluminescence Plus kit purchased from Proteintech and quantified with the Quantity One Software (BioRad) following a wash with TBST.

2.9. Statistical analysis

Excel, SPSS (version 21), or Prism 8 (GraphPad software) were employed for statistical analyses. Differences between treatment groups and control group were evaluated by Student's t-test. Two-tailed unpaired Student's t tests were used to determine the statistical significance of comparison tests between the two groups (* $p < 0.05$, ** $p < 0.01$, *** $p < 0.001$ and **** $p < 0.0001$). The mean standard deviation was used to report statistical data.

3. Results

3.1. TLSs exist in ovarian cancer patients, and high TLS scores predicts a good prognosis

T and B cell immunofluorescence staining was used to identify TLSs in tissue slides as true TLSs (Fig. 1) [17,25,26]. This indicated that the components of lymphocyte aggregates observed in HE-stained sections were consistent with the structural composition of TLSs. The formation of TLSs in the ovarian cancer tissues of patients was analyzed by observing HE staining images. Then, we evaluated the expression of TLS from three aspects: the number of TLS (the long diameter of a polymer less than 100 μm was statistically half of TLS), the cell density of each TLS (sparse = 1, medium = 2, dense = 3) and the ratio of TLS area to the whole slice. Finally, these three indicators were combined to obtain the final score. The density score of each TLS was added to obtain the total density score, which was multiplied by the ratio of the TLS area to the total slice area to obtain the final score. Subsequently, we analyzed the correlation between TLS, patient pathological parameters, and overall survival and found that older age, later FIGO stage, presence of vascular cancer thrombus, and low TLS scores all led to poor prognosis (Table 1). We further plotted the K-M survival curve of patients with OS, and the findings demonstrated that patients with high TLS scores had a better prognosis than individuals with low TLS scores. Stratified analysis also obtained the same result in patients with no lymph node metastasis or thrombotic metastasis (Fig. 2A–B). Finally, multifactor regression model analysis showed that TLS was a positive prognostic factor and a protective independent prognostic factor for ovarian cancer patients after surgery (Table 2).

3.2. CDK4/6i can promote the formation of TLSs in ovarian cancer

We examined the impact of CDK4/6i on TLS production by establishing an animal model of ovarian cancer. Female C57BL/6 mice aged 6 weeks were intraperitoneally injected with 5×10^6 ID8-Luc cells and monitored for tumor formation using IVIS every week. Tumor-bearing mice were randomly separated into four groups and treated with PBS, CDK4/6i monotherapy, PD1 monoclonal antibody, and the combination of CDK4/6i and PD1 antibody after one month. Mice in the combination group ($n = 6$) were given abemaciclib (50 mg/kg), 1 time/d, along with α -PD-1, 200 $\mu\text{g}/\text{once}$, 1 time/3d, and mice in the abemaciclib group ($n = 6$) were given

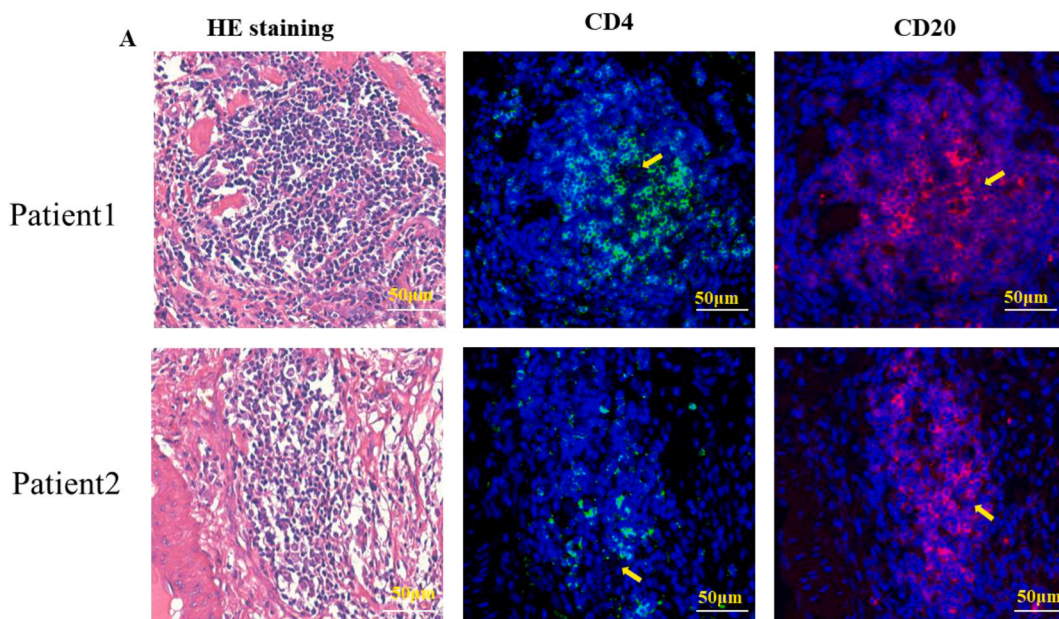


Fig. 1. Identification of TLSs in ovarian cancer tissues. (A) HE staining and corresponding immunofluorescence staining of CD4⁺ T cells and CD20⁺ B cells in tissue sections of ovarian cancer patients.

Table 1
Relationship between TLS, pathological parameters and overall survival.

Clinicopathologic parameter	Number of cases	Prognosis	Mean survival time	Log-Rank	P value
	(n = 196)	Death	(Month)	X ²	
Age (years)				10.952	0.001
≤65	168	37	32.178		
>65	28	14	27.071		
Tumor size (cm)				0.504	0.478
≤5	26	8	29.885		
>5	170	43	31.687		
FIGO staging				11.119	0.011
I	40	5	34.293		
II	19	4	31.737		
III	124	35	31.153		
IV	13	7	25.077		
Lymph node metastasis				2.462	0.117
Yes	81	26	30.616		
No	115	25	32.033		
Intravascular cancer thrombus				5.052	0.025
Yes	20	9	27.150		
No	176	42	31.936		
TLS				6.030	0.014
High	112	22	32.928		
Low	84	29	29.474		

Notes: Values in bold signify $P < 0.05$.

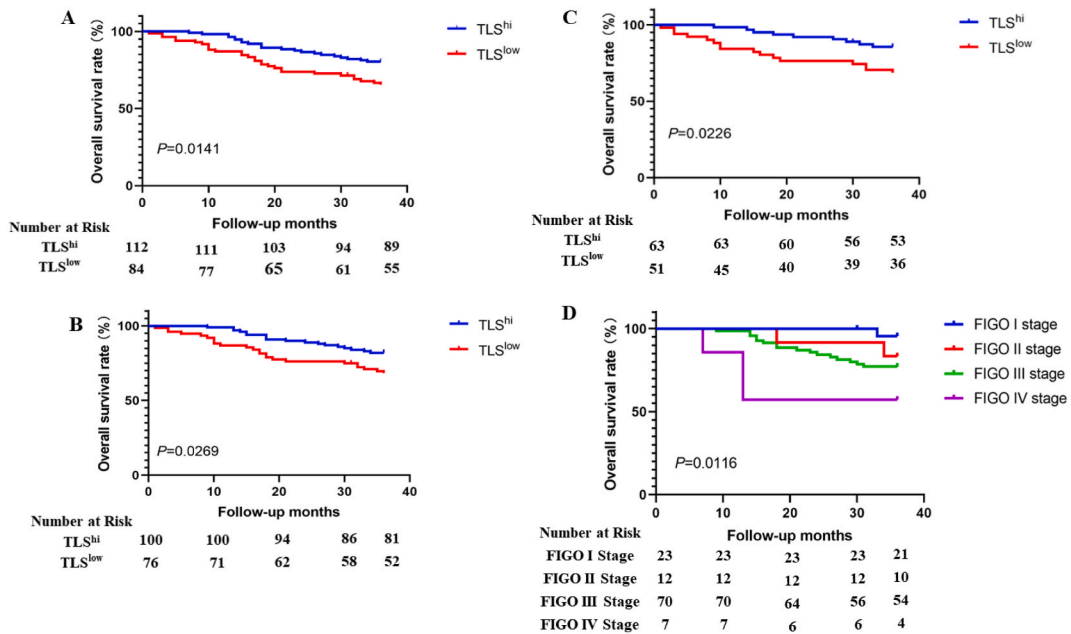


Fig. 2. Kaplan-Meier survival curve between TLS and OS. Relationship between TLS expression and OS in ovarian cancer patients (A). The relationship between the expression of TLSs and OS in patients without vascular thrombi (B). Relationship between TLS expression and OS in patients without lymph node metastasis (C). Relationship between stage and OS in ovarian cancer patients with high TLS expression (D).

abemaciclib (50 mg/kg), 1 time/d, and α -PD-1 group mice ($n = 6$) were given α -PD-1, 200 μ g/dose, 1 time/3d. PBS control group mice ($n = 6$) were given PBS as a negative control. Changes in tumor size in each group were observed by IVIS, and it was found that the combined treatment group could significantly inhibit tumor growth by day 7 of treatment (Fig. 3A–B). On the 10th day of treatment, we dissected the mice to obtain tumor tissue. HE-stained slices of mouse tumor tissue revealed that the formation of TLSs was considerably higher in the combination therapy group than in the control group (Fig. 3C–D). Combined treatment significantly increased the secretion of the chemokines CCL21, CXCL13, and VEGFC in the serum of mice, as determined by ELISA (Fig. 3E–G). Our previous study proved that CDK4/6i can promote T cells and B cells to gather into clusters and contact closely in an in vivo model [16]. In addition, increases in CCL21, CXCL13, and VEGFC were detected in the treated cell supernatant when ID8 cell lines were treated with CDK4/6i [16]. CCL21, CXCL13, and VEGFC are considered to be key chemokines in TLS formation [21]. These factors can

Table 2
Cox analysis of factors associated with an increased risk of tumor progression.

Clinicopathologic parameter	Univariate COX analysis			Multivariate COX analysis		
	HR	95%CI	P value	HR	95%CI	P value
Age ($\leq 65 / > 65$)	2.703	1.460–5.003	0.002	2.796	1.496–5.224	0.001
Tumor size (cm) ($\leq 5 \text{cm} / > 5 \text{cm}$)	0.762	0.358–1.621	0.481			
FIGO staging						
I	1	Reference		1	Reference	
II	1.815	0.487–6.760	0.374	2.153	0.574–8.076	0.256
III	2.490	0.975–6.356	0.056	2.239	0.823–6.093	0.115
IV	5.968	1.890–18.845	0.002	4.250	1.177–15.343	0.027
Lymph node metastasis (Yes/No)	1.544	0.892–2.675	0.121	1.079	0.587–1.984	0.807
Intravascular cancer thrombus (Yes/No)	2.230	1.084–4.585	0.029	1.628	0.717–3.695	0.244
TLS (High/Low)	0.507	0.291–0.883	0.016	0.505	0.289–0.883	0.017

Notes: Values in bold signify $P < 0.05$.

mediate the formation of mature TLS T-cell and B-cell domains. The secretion of VEGFC is closely related to HEV formation in TLS [20]. Therefore, our results confirm that CDK4/6i can indeed promote the formation of TLSs in ovarian cancer.

3.3. High-throughput RNA sequencing revealed that CDK4/6i can downregulate SCD1

To investigate the mechanism by which CDK4/6i affects TLS formation, we performed high-throughput transcriptome sequencing analysis using tumor tissues from mice. Comparing the combined treatment group with the control group, differential gene expression analysis revealed that 245 genes were downregulated and 423 genes were upregulated (Fig. 4C). Compared with the PBS group, 86 upregulated genes and 234 downregulated genes were found in CDK4/6i group (Fig. 4A). 575 upregulated genes and 260 downregulated genes were found in the α -PD-1 group (Fig. 4B). In addition, we conducted cluster analysis on differentially expressed genes and found that the regulation pattern of gene expression in the same group was similar, which may participate in a similar biological process (Fig. 4D).

The combined group and the control group's differential genes were analyzed for GO enrichment. The downregulated differential genes were mainly enriched in pathways related to metabolic processes, including lipid metabolism and fatty acid metabolism (Fig. 4E). Any cell needs energy metabolism to perform its function and survive, and T cells are no exception. Glycolysis is the main metabolic pathway required after T cell activation, and lipid metabolism plays an important role in T cell proliferation and effector memory T cell differentiation [27]. Some important regulatory molecules of T cell differentiation have also been shown to be involved in metabolic pathways, such as T cell costimulatory factor, glucose transporter 1, and interferon regulatory factor 4 [28]. The upregulated differential gene enrichment pathways include positive regulation of T-cell-mediated cytotoxicity, positive regulation of T-cell activation, immune system processes, and antigen processing and presentation via MHCII-like peptide antigens (Fig. 4F). These pathways are directly related to T cell function. The above pathways were closely related to immune metabolism.

We obtained the intersection gene set of different genes in each group by Venn diagram (Fig. 4G–H). The downregulated genes included Pygl, Ighv1-5, Iglv2, Ehhadh, Papss2, Scd1, Hsd11b1, Cat, Fmo5, Dpyd, Tmem82, Aldh111, Fah, Agt, Paqr9, AI507597, Gm15756, Hacl1, Pemt, Lpl, and Gstz1 (Fig. 4I). After reviewing previous studies, we found that SCD1 was the most significantly reduced gene associated with tumor immunity.

Stearoyl-CoA desaturase 1 (SCD1) is a vital enzyme in the metabolism of fatty acids and a rate-limiting enzyme in the synthesis of monounsaturated fatty acids (MUFAs) [29,30]. Accumulating evidence indicates that SCD1, as a central regulator of metabolism and signal transduction, controls cell metabolism and cell cycle progression and is a key factor leading to cancer development, which plays a critical role in various tumors [30,31]. SCD1 may be a potential therapeutic opportunity and future direction [32]. Studies have found that SCD1 inhibitors can enhance the induction and aggregation of antitumor CD8⁺ T cells in tumors. SCD1 inhibitors or SCD1 gene knockout can synergize with PD-1 antibodies to suppress tumor growth in mouse models [33]. As a consequence, downregulation of the SCD1 gene may be the key process by which CDK4/6i promotes the formation of TLSs.

3.4. CDK4/6i can promote the formation of TLS by decreasing SCD1

According to several studies, SCD1 inhibition increases the expression of CCL4 in mouse and human cancer cells while decreasing the expression of its downstream component, ATF3 [34–36]. Through the recruitment of DCs into tumors, which in turn triggers the development of tumor antigen-specific CD8⁺ T cells and supports the infiltration of CD8⁺ effector T cells into the tumor, chemokines such as CCL4 have been reported to play a significant role in the development of a T cell-inflamed TME [37]. Therefore, we verified the transcriptome sequencing results and detected the gene expression levels of ATF3 and CCL4 in tumor tissues of mice in each group using quantitative real-time PCR (Fig. 5A–C). PD1 antibody and CDK4/6i therapy together dramatically decreased the expression of SCD1 in mouse ovarian cancer tissues. Meanwhile, the downregulation of SCD1 inhibited the expression of ATF3 and upregulated the expression level of CCL4. The same results were obtained for IHC (Fig. 5D–G). In addition, the results were verified by western blotting (Fig. 5I–L). We also further analyzed the expression of CD8⁺ T cells in mouse ovarian cancer tissues and found that CD8⁺ T cells in the combined treatment group of CDK4/6i and PD1 antibody were significantly increased in mouse tumor tissues (Fig. 5D, H). To further

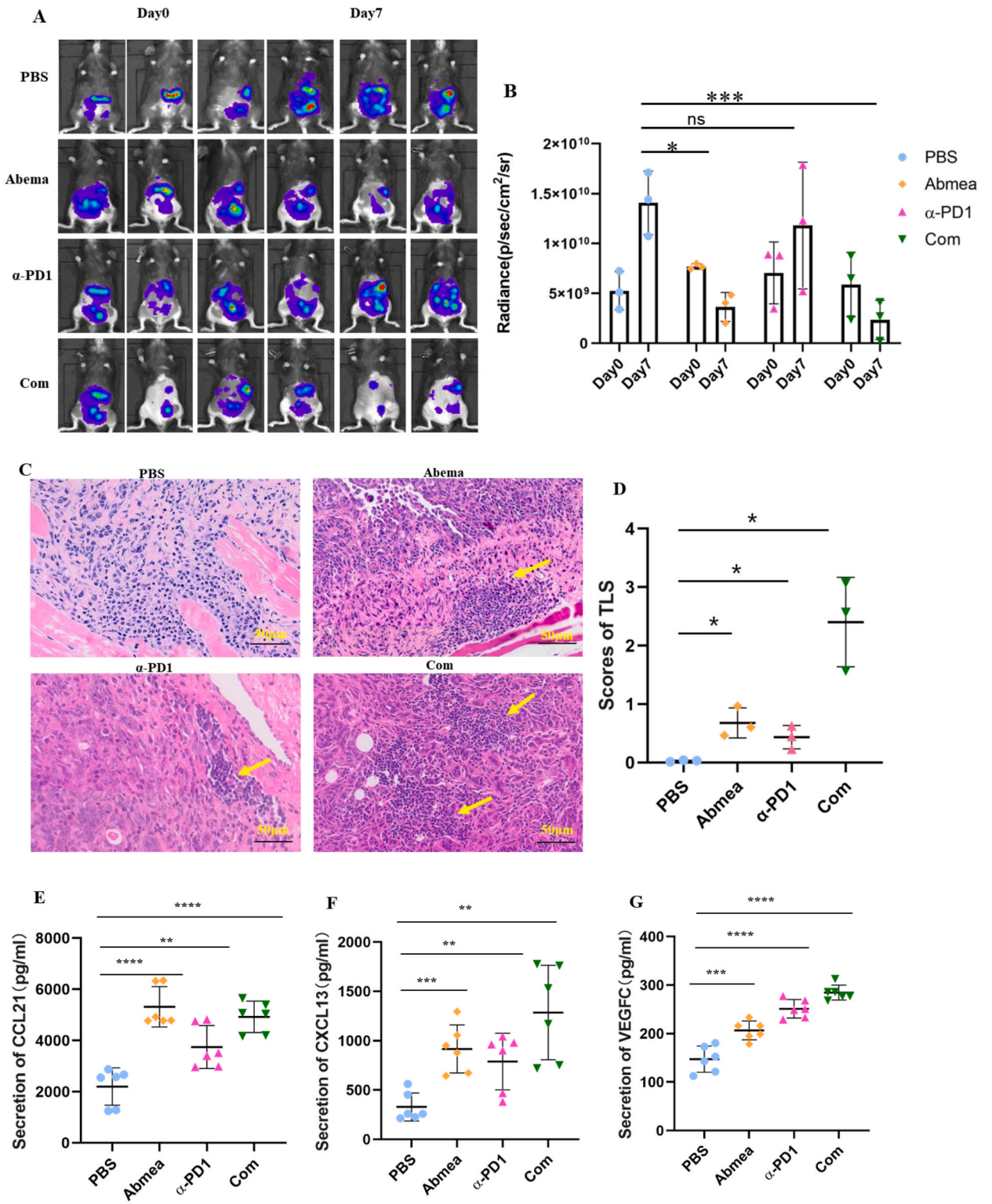
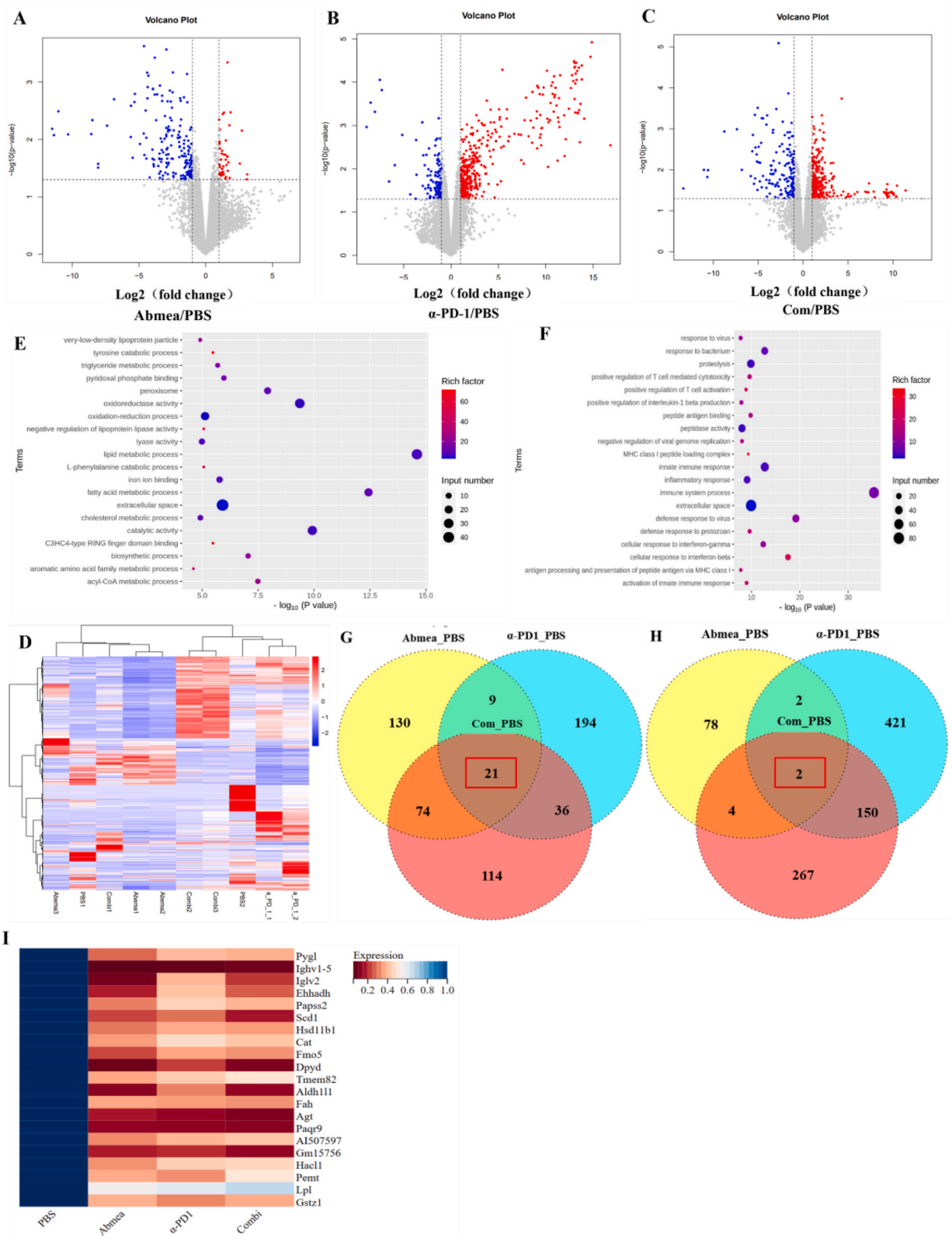


Fig. 3. Changes in tumor size in different treatment groups (A–B). Scores of TLS in tumor tissues of mice in different treatment groups (C–D). Expression of CCL21 (E), CXCL13 (F) and VEGFC (G) in the serum of mice in different treatment groups.



(caption on next page)

Fig. 4. Volcanic maps of differentially expressed genes between control and CDK4/6i groups (A). Volcanic maps of differentially expressed genes between control and α -PD1 groups (B). Volcanic maps of differentially expressed genes between control and Combined treatment groups (C). The hierarchical clustering analysis was used to classify different regulation patterns of gene expression, and the regulation patterns of gene expression in the same group were similar (D). GO enrichment analyses of downregulated (E) and upregulated (F) genes between combination group and control group. Venn diagram displayed downregulated and upregulated intersecting genes (G, H). The scale of fold change was used to make heat map to display the intersection genes between three treatment groups and the control group (I).

investigate the influence of SCD1 expression on TLSs, we analyzed the correlation between SCD1 expression and TLS expression in ovarian cancer patients. The results revealed that the expression of SCD1 was negatively correlated with TLS (Fig. 6A–B). These results suggested that CDK4/6i can promote the aggregation of CD8⁺ T cells by regulating SCD1 and its regulatory molecules ATF3, and CCL4 and ultimately form local TLSs in ovarian cancer.

4. Discussion

At present, anti-PD-1/PD-L1 treatment has become a very powerful therapeutic strategy in the history of immunotherapy [38]. However, in ovarian cancer, this antitumor effect is limited [3]. Therefore, it is urgent to develop more effective combination therapies to enhance their effects and obtain long-term benefits. Studies have shown that CDK4/6 inhibitors have the ability to increase the degree of T cell infiltration in tumor tissues and ultimately regulate the immune microenvironment [6–8]. Our previous results confirmed that CDK4/6i has a synergistic effect with an anti-PD1 antibody in ovarian cancer, and TLSs were observed in ovarian cancer tissues after CDK4/6i treatment. Tertiary lymphatic structure is a special immune polymer that appears in tumors, and its presence has been found in many studies to be associated with favorable prognosis [18]. TLS structures are hypothesized to actively affect antitumor immune activity rather than simply serving as a proxy indication of a rapid immune response.

In this study, through the data analysis of clinical patients in the first section, we discovered that TLS exists in the tissues of ovarian cancer patients and is a positive predictor of the postoperative prognosis of patients. The multifactor Cox model also showed that TLS was a protective independent prognostic factor, which has been shown in other cancer types [17,39]. With the deepening study of TLSs, they have been identified within a variety of human cancers at various phases of the disease in both primary and metastatic lesions, but their presence varies greatly between cancer types and patients [20,40]. The cellular components of TLSs and their location within tumors exhibit significant heterogeneity as well. This may affect the overall impact on antitumor immunity and prognosis. Activated T cells and B cells in mature TLSs can produce synergistic effects to kill tumor cells and promote a sustained immune response within the tumor, which is an important tumor immune mechanism. This may explain why ovarian cancer patients with high TLS expression had a better prognosis. However, our stratified analysis results indicated that high scores of TLSs only in patients without lymph node metastasis and without vascular cancer thrombi had a good prognosis. This suggested that high expression of TLSs could not change the adverse effects of lymph node metastasis and vascular cancer thrombi. In addition, it may also have to do with the nature of TLS. Immature TLSs play little role in antitumor immunity [41,42]. For instance, the absence of TLS-associated dendritic cells negates the benefit of a high CD8⁺ T cell density within a tumor [43,44]. Generally, in view of the potential value of TLSs in prognosis and cancer immunotherapy, exploring therapeutic strategies to induce the formation of TLSs may effectively improve patients' response to tumor immunotherapy and improve the clinical manifestations of ovarian cancer. Both treatment and prognosis are of great value.

Our previous study found that CDK4/6i could promote the aggregation of T cells and B cells in mouse ovarian cancer, which may be associated with TLS formation. CDK4/6i combined with PD1 antibody had a significant effect on mouse ovarian cancer [16]. We speculated that CDK4/6i stimulated the development of local TLSs in ovarian cancer, thus improving the immune microenvironment. To further study the role of CDK4/6i in the formation of TLSs, we established an animal model of ovarian cancer and observed the same results as previous research. Furthermore, we found that the secretion of CXCL13 [45], CCL21, and VEGFC [46,47] in the serum of mice in the combined treatment group was significantly increased. CXCL13, CCL21, and VEGFC are key factors in TLS formation. The chemokine CXCL13 mediates the recruitment of B cells to tumors and is essential for TLSs. These factors can co-induce lymphocyte expression of LT α 1 β 2, recruit lymphocytes from neighboring HEVs and mediate the formation of mature TLS T cell and B cell domains. The secretion of VEGFC is closely related to HEV formation in TLS [20]. These results further suggested that CDK4/6i can promote the formation of TLSs in mouse ovarian cancer.

After observing that CDK4/6i stimulated TLS formation, transcriptome sequencing was performed on animal tissues to further explore the underlying mechanism. *SCD1* decreased in all treatment groups compared to the control group, according to the results of the RNA sequencing. Immunohistochemistry, quantitative real-time PCR, and western blotting were used to confirm the results. It has been reported that the expression and activity of SCD1 is bidirectionally regulated by Wnt/ β -catenin signaling, and activation of Wnt/ β -catenin signaling inhibits CCL4 production through ATF3 activation [34,36,48–50]. Researchers have demonstrated that SCD1 regulates the production of CCL4 in a variety of tumor cell lines via the β -catenin-ATF3 axis [33]. Similarly, our findings showed that SCD1 inhibition suppresses the expression of ATF3 and enhances the expression of CCL4 in mouse ovarian cancer. By attracting DCs into tumors, which then excite tumor antigen-specific CD8⁺ T cells and increase tumor-infiltrating CD8⁺ effector T cells, CCL4 plays a critical role in the formation of a T cell-inflamed TME [37]. We also conducted immunohistochemical experiments to detect the expression of CD8⁺ T cells in mouse ovarian tissues. The findings demonstrated that the combined group's CD8⁺ T cell count increased. Therefore, we think the SCD1 and its regulatory molecules ATF3 and CCL4 were involved in the mechanism of CDK4/6i by which CDK4/6i functions. To further reveal the correlation between SCD1 and TLS, we examined the variations in SCD1 gene expression in

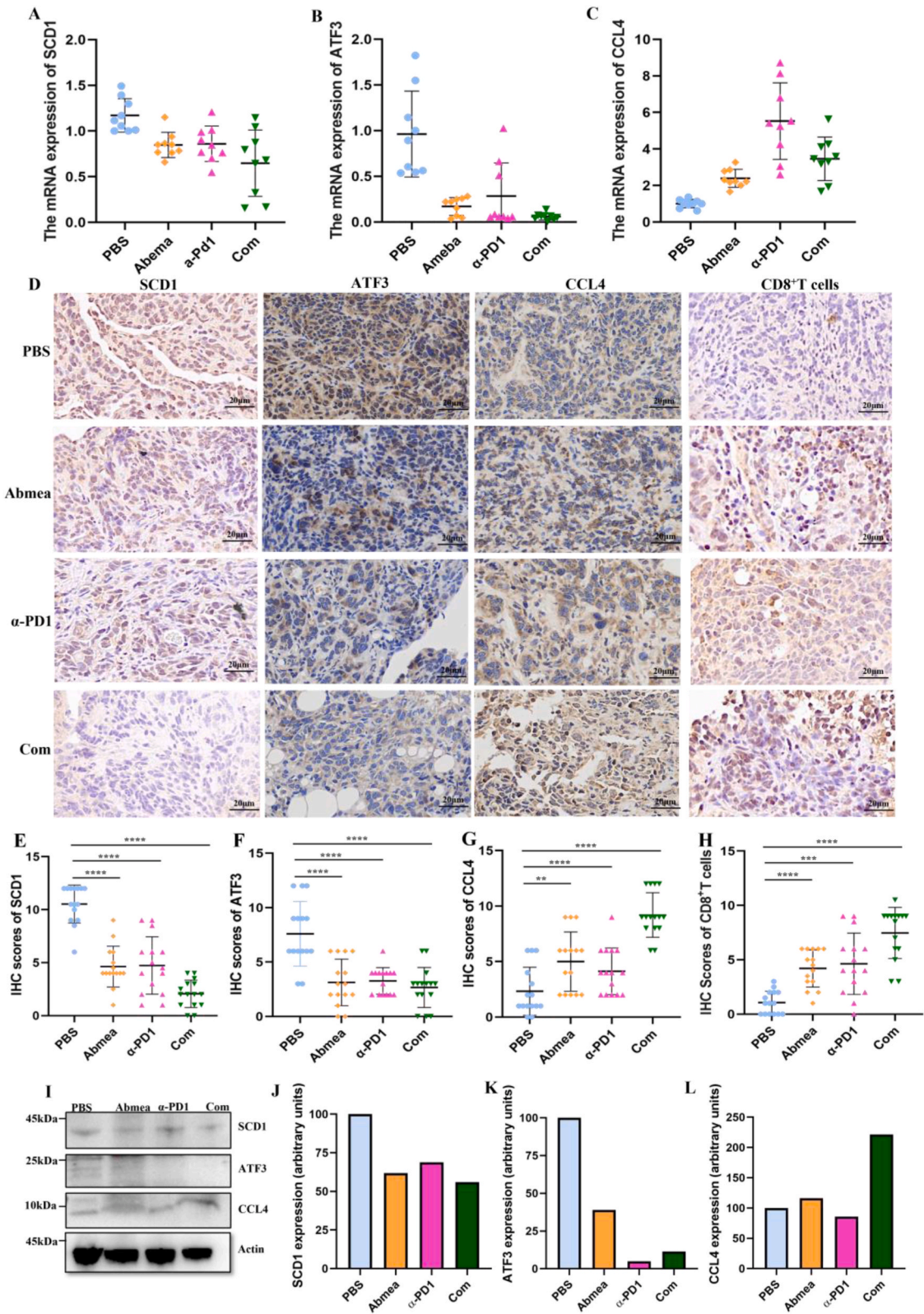


Fig. 5. RT-QPCR showed the expression of SCD1 and its regulatory genes ATF3 and CCL4 expression in tumor tissues of mice (n = 3) (A–C). The expression of SCD1, ATF3, CCL4 and infiltration of CD8⁺T cells were detected in tumor tissues of mice in different treatment groups by IHC (D–H). The protein levels of SCD1, ATF3 and CCL4 in mouse tumor tissues were detected by western blotting (I–L).

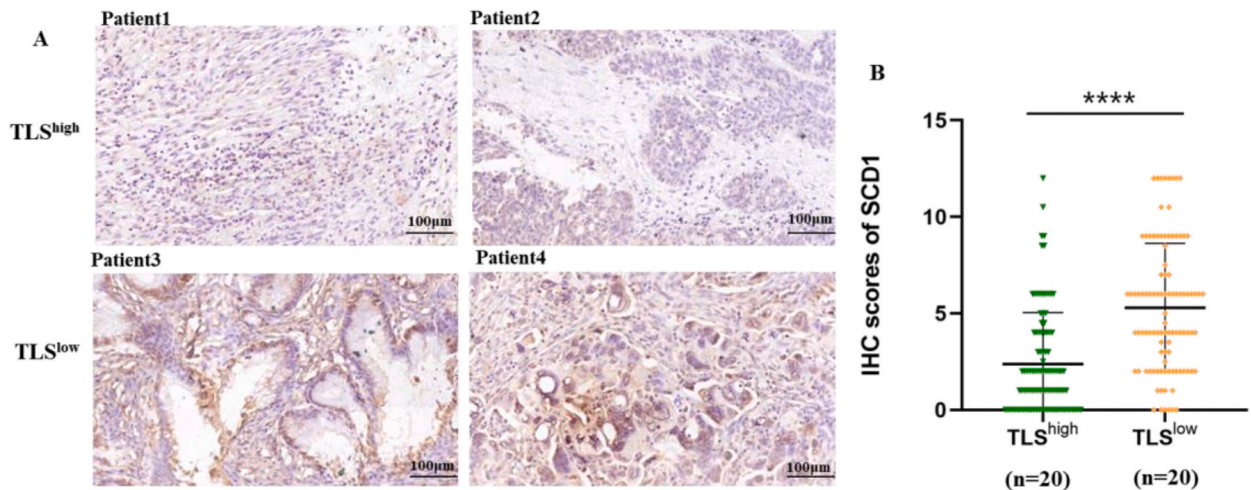


Fig. 6. IHC results displayed correlation analysis between SCD1 expression and TLS score in ovarian cancer patients (A–B).

the tissues of patients with high and low TLS expression. Individuals with high TLS expression also had reduced SCD1 expression. These results indicate a negative correlation between the expression of SCD1 and TLS. Therefore, we inferred that CDK4/6i may through modulated the SCD1 and its regulatory molecules to promote an increase in T cells in tumor tissues and ultimately lead to the formation of TLSs.

5. Conclusion

In conclusion, our research demonstrated that TLS was a stand-alone protective factor for people with ovarian cancer. CDK4/6i can promote the formation of TLSs in ovarian cancer. Moreover, it was found that this may be realized through the mechanism of reducing SCD1, thereby inhibiting ATF3 and upregulating CCL4. More *in vivo* studies are needed to confirm this mechanism and deep studies can be conducted if possible. Finally, our study provides a new combination therapy idea and strategy for immunotherapy. It can also be a theoretical basis for the application of CDK4/6i in ovarian cancer.

Author contribution statement

Wangyou Feng: Performed the experiments; Wrote the paper.

Dongbo Jiang: Conceived and designed the experiments.

Ying Xu: Analyzed and interpreted the data.

Yuanfeng Li; Lin Chen; Minye Zhao; Yujie Shen; Wenjing Liao: Contributed reagents, materials, analysis tools or data.

Hong Yang; Jia Li: Conceived and designed the experiments; Contributed reagents, materials, analysis tools or data.

Data availability statement

Data associated with this study has been deposited at the GEO database under the accession number GSE234106.

Funding

This work was supported by the National Nature Science Foundation of China (grant number 82172993), the Natural Science Basic Research Plan in Shaanxi Province of China (grant number 2022JQ-977) and the Key R&D plan of Shaanxi Province (grant number 2023-YBSF-484).

Declaration of competing interest

The authors declare that they have no known competing financial interests or personal relationships that could have appeared to influence the work reported in this paper.

Acknowledgments

We acknowledge the use of the facility of the Airforce Military Medical University.

Appendix A. Supplementary data

Supplementary data to this article can be found online at <https://doi.org/10.1016/j.heliyon.2023.e19760>.

References

- [1] S. Lheureux, C. Gourley, I. Vergote, A.M. Oza, Epithelial ovarian cancer, *Lancet* 393 (2019) 1240–1253, [https://doi.org/10.1016/S0140-6736\(18\)32552-2](https://doi.org/10.1016/S0140-6736(18)32552-2).
- [2] D.B. Doroshov, S. Bhalla, M.B. Beasley, L.M. Sholl, K.M. Kerr, S. Gnjatic, et al., PD-L1 as a biomarker of response to immune-checkpoint inhibitors, *Nat. Rev. Clin. Oncol.* 18 (2021) 345–362, <https://doi.org/10.1038/s41571-021-00473-5>.
- [3] J. Hamanishi, M. Mandai, T. Ikeda, M. Minami, A. Kawaguchi, T. Murayama, et al., Safety and antitumor activity of anti-PD-1 antibody, nivolumab, in patients with platinum-resistant ovarian cancer, *J. Clin. Oncol.* 33 (2015) 4015–4022, <https://doi.org/10.1200/JCO.2015.62.3397>.
- [4] J. Hamanishi, M. Mandai, M. Iwasaki, T. Okazaki, Y. Tanaka, K. Yamaguchi, et al., Programmed cell death 1 ligand 1 and tumor-infiltrating CD8+ T lymphocytes are prognostic factors of human ovarian cancer, *Proc. Natl. Acad. Sci. U.S.A.* 104 (2007) 3360–3365, <https://doi.org/10.1073/pnas.0611533104>.
- [5] Z.A. Cooper, V.R. Juneja, P.T. Sage, D.T. Frederick, A. Piris, D. Mitra, et al., Response to BRAF inhibition in melanoma is enhanced when combined with immune checkpoint blockade, *Cancer Immunol. Res.* 2 (2014) 643–654, <https://doi.org/10.1158/2326-6066.CIR-13-0215>.
- [6] D.A. Schaer, R.P. Beckmann, J.A. Dempsey, L. Huber, A. Forest, N. Amaladas, et al., The CDK4/6 inhibitor abemaciclib induces a T cell inflamed tumor microenvironment and enhances the efficacy of PD-L1 checkpoint blockade, *Cell Rep.* 22 (2018) 2978–2994, <https://doi.org/10.1016/j.celrep.2018.02.05>.
- [7] J. Deng, E.S. Wang, R.W. Jenkins, S. Li, R. Dries, K. Yates, et al., CDK4/6 inhibition augments antitumor immunity by enhancing T-cell activation, *Cancer Discov.* 8 (2018) 216–233, <https://doi.org/10.1158/2159-8290.CD-17-0915>.
- [8] S. Goel, M.J. DeCristo, A.C. Watt, H. BrinJones, J. Sceneay, B.B. Li, et al., CDK4/6 inhibition triggers anti-tumour immunity, *Nature* 548 (2017) 471–475, <https://doi.org/10.1038/nature23465>.
- [9] J. Zhang, X. Bu, H. Wang, Y. Zhu, Y. Geng, N.T. Nihira, et al., Cyclin D-CDK4 kinase destabilizes PD-L1 via cullin 3-SPOP to control cancer immune surveillance, *Nature* 553 (2018) 91–95, <https://doi.org/10.1038/nature25015>.
- [10] B. O’Leary, R.S. Finn, N.C. Turner, Treating cancer with selective CDK4/6 inhibitors, *Nat. Rev. Clin. Oncol.* 13 (2016) 417–430, <https://doi.org/10.1038/nrclinonc.2016.26>.
- [11] N.C. Turner, D.J. Slamon, J. Ro, I. Bondarenko, S.A. Im, N. Masuda, et al., Overall survival with palbociclib and fulvestrant in advanced breast cancer, *N. Engl. J. Med.* 379 (2018) 1926–1936, <https://doi.org/10.1056/NEJMoa1810527>.
- [12] K.K. Kim, Expression of cyclin D1 and CDK4 in DMBA-induced rat ovarian cancer, *Cancer. Res. Treat.* 33 (2001) 229–235, <https://doi.org/10.4143/crt.2001.33.3.229>.
- [13] G.E. Konecny, B. Winterhoff, T. Kolarova, J. Qi, K. Manivong, J. Dering, et al., Expression of p16 and retinoblastoma determines response to CDK4/6 inhibition in ovarian cancer, *Clin. Cancer Res.* 17 (2011) 1591–1602, <https://doi.org/10.1158/1078-0432.CCR-10-2307>.
- [14] G.E. Konecny, A. Jatoi, J.K. Burton, J. Paroly, J.A. Glaspy, S.C. Dowdy, et al., A multicenter open-label phase II study of the efficacy and safety of palbociclib a cyclin-dependent kinases 4 and 6 inhibitor in patients with recurrent ovarian cancer, 5557-5557, *J. Clin. Oncol.* (2016), https://doi.org/10.1200/JCO.2016.34.15_suppl.5557.
- [15] A. Patnaik, L.S. Rosen, S.M. Tolaney, A.W. Tolcher, J.W. Goldman, L. Gandhi, et al., Efficacy and safety of abemaciclib, an inhibitor of CDK4 and CDK6, for patients with breast cancer, non-small cell lung cancer, and other solid tumors, *Cancer Discov.* 6 (2016) 740–753, <https://doi.org/10.1158/2159-8290.CD-16-0095>.
- [16] Q.F. Zhang, J. Li, K. Jiang, R. Wang, J.L. Ge, H. Yang, et al., CDK4/6 inhibition promotes immune infiltration in ovarian cancer and synergizes with PD-1 blockade in a B cell-dependent manner, *Theranostics* 10 (2020) 10619–10633, <https://doi.org/10.7150/thno.44871>.
- [17] R. Cabrita, M. Lauss, A. Sanna, M. Donia, M. Skaarup Larsen, S. Mitra, et al., Tertiary lymphoid structures improve immunotherapy and survival in melanoma, *Nature* 577 (2020) 561–565, <https://doi.org/10.1038/s41586-019-1914-8>.
- [18] B.A. Helmink, S.M. Reddy, J. Gao, S. Zhang, R. Basar, R. Thakur, et al., B cells and tertiary lymphoid structures promote immunotherapy response, *Nature* 577 (2020) 549–555, <https://doi.org/10.1038/s41586-019-1922-8>.
- [19] F. Petitprez, A. de Reynies, E.Z. Keung, T.W. Chen, C.M. Sun, J. Calderaro, et al., B cells are associated with survival and immunotherapy response in sarcoma, *Nature* 577 (2020) 556–560, <https://doi.org/10.1038/s41586-019-1906-8>.
- [20] C. Sautes-Fridman, F. Petitprez, J. Calderaro, W.H. Fridman, Tertiary lymphoid structures in the era of cancer immunotherapy, *Nat. Rev. Cancer* 19 (2019) 307–325, <https://doi.org/10.1038/s41568-019-0144-6>.
- [21] C. Sautes-Fridman, W.H. Fridman, TLS in tumors: what lies within, *Trends Immunol.* 37 (2016) 1–2, <https://doi.org/10.1016/j.it.2015.12.001>.
- [22] A. Johansson-Percival, B. He, Z.J. Li, A. Kjellen, K. Russell, J. Li, et al., De novo induction of intratumoral lymphoid structures and vessel normalization enhances immunotherapy in resistant tumors, *Nat. Immunol.* 18 (2017) 1207–1217, <https://doi.org/10.1038/ni.3836>.
- [23] A. Mortazavi, B.A. Williams, K. McCue, L. Schaeffer, B. Wold, Mapping and quantifying mammalian transcriptomes by RNA-Seq, *Nat. Methods* 5 (2008) 621–628, <https://doi.org/10.1038/nmeth.1226>.
- [24] S. Tarazona, F. Garcia-Alcalde, J. Dopazo, A. Ferrer, A. Conesa, Differential expression in RNA-seq: a matter of depth, *Genome Res.* 21 (2011) 2213–2223, <https://doi.org/10.1101/gr.124321.111>.
- [25] X. Hu, X.S. Liu, A high-resolution view of intra-tumoral B cell immunity, *Immunity* 55 (2022) 387–389, <https://doi.org/10.1016/j.immuni.2022.02.009>.
- [26] J. Wang, D. Jiang, X. Zheng, W. Li, T. Zhao, D. Wang, et al., Tertiary lymphoid structure and decreased CD8(+) T cell infiltration in minimally invasive adenocarcinoma, *iScience* 25 (2022), 103883, <https://doi.org/10.1016/j.isci.2022.103883>.
- [27] A. Sharabi, G.C. Tsokos, T cell metabolism: new insights in systemic lupus erythematosus pathogenesis and therapy, *Nat. Rev. Rheumatol.* 16 (2020) 100–112, <https://doi.org/10.1038/s41584-019-0356-x>.
- [28] G.R. Bantug, L. Galluzzi, G. Kroemer, C. Hess, The spectrum of T cell metabolism in health and disease, *Nat. Rev. Immunol.* 18 (2018) 19–34, <https://doi.org/10.1038/nri.2017.99>.
- [29] Y. Bai, J.G. McCoy, E.J. Levin, P. Sobrado, K.R. Rajashankar, B.G. Fox, et al., X-ray structure of a mammalian stearyl-CoA desaturase, *Nature* 524 (2015) 252–256, <https://doi.org/10.1038/nature14549>.
- [30] L. Hodson, B.A. Fielding, Stearyl-CoA desaturase: rogue or innocent bystander? *Prog. Lipid Res.* 52 (2013) 15–42, <https://doi.org/10.1016/j.plipres.2012.08.002>.
- [31] B. Peck, Z.T. Schug, Q. Zhang, B. Dankworth, D.T. Jones, E. Smethurst, et al., Inhibition of fatty acid desaturation is detrimental to cancer cell survival in metabolically compromised environments, *Cancer Metab.* 4 (2016) 6, <https://doi.org/10.1186/s40170-016-0146-8>.
- [32] R.A. Igal, Stearyl CoA desaturase-1: new insights into a central regulator of cancer metabolism, *Biochim. Biophys. Acta* 1861 (2016) 1865–1880, <https://doi.org/10.1016/j.bbali.2016.09.009>.
- [33] Y. Katoh, T. Yaguchi, A. Kubo, T. Iwata, K. Morii, D. Kato, et al., Inhibition of Stearyl-CoA desaturase 1 (SCD1) enhances the antitumor T cell response through regulating beta-catenin signaling in cancer cells and ER stress in T cells and synergizes with Anti-PD-1 antibody, *J. Immunother. Cancer.* (2022), 10.101136/jitc-2022-004616.
- [34] C.H. Khuu, R.M. Barrozo, T. Hai, S.L. Weinstein, Activating transcription factor 3 (ATF3) represses the expression of CCL4 in murine macrophages, *Mol. Immunol.* 44 (2007) 1598–1605, <https://doi.org/10.1016/j.molimm.2006.08.006>.

- [35] D. Mauvoisin, C. Charfi, A.M. Lounis, E. Rassart, C. Mounier, Decreasing stearoyl-CoA desaturase-1 expression inhibits beta-catenin signaling in breast cancer cells, *Cancer Sci.* 104 (2013) 36–42, <https://doi.org/10.1111/cas.12032>.
- [36] S. Spranger, R. Bao, T.F. Gajewski, Melanoma-intrinsic beta-catenin signalling prevents anti-tumour immunity, *Nature* 523 (2015) 231–235, <https://doi.org/10.1038/nature14404>.
- [37] H. Harlin, Y. Meng, A.C. Peterson, Y. Zha, M. Tretiakova, C. Slingluff, et al., Chemokine expression in melanoma metastases associated with CD8+ T-cell recruitment, *Cancer Res.* 69 (2009) 3077–3085, <https://doi.org/10.1158/0008-5472.CAN-08-2281>.
- [38] A. Ribas, J.D. Wolchok, Cancer immunotherapy using checkpoint blockade, *Science* 359 (2018) 1350–1355, <https://doi.org/10.1126/science.aar4060>.
- [39] H.J. Lee, J.Y. Kim, I.A. Park, I.H. Song, J.H. Yu, J.H. Ahn, et al., Prognostic significance of tumor-infiltrating lymphocytes and the tertiary lymphoid structures in HER2-positive breast cancer treated with adjuvant trastuzumab, *Am. J. Clin. Pathol.* 144 (2015) 278–288, <https://doi.org/10.1309/AJCPXUYDYZORZ3G>.
- [40] E.J. Colbeck, A. Ager, A. Gallimore, G.W. Jones, Tertiary lymphoid structures in cancer: drivers of antitumor immunity, immunosuppression, or bystander sentinels in disease? *Front. Immunol.* 8 (2017) 1830, <https://doi.org/10.3389/fimmu.2017.01830>.
- [41] A. Cipponi, M. Mercier, T. Seremet, J.F. Baurain, I. Theate, J. van den Oord, et al., Neogenesis of lymphoid structures and antibody responses occur in human melanoma metastases, *Cancer Res.* 72 (2012) 3997–4007, <https://doi.org/10.1158/0008-5472.CAN-12-1377>.
- [42] S.R. Selitsky, L.E. Mose, C.C. Smith, S. Chai, K.A. Hoadley, D.P. Dittmer, et al., Prognostic value of B cells in cutaneous melanoma, *Genome Med.* 11 (2019) 36, <https://doi.org/10.1186/s13073-019-0647-5>.
- [43] F. Posch, K. Silina, S. Leibl, A. Mundlein, H. Moch, A. Siebenhuner, et al., Maturation of tertiary lymphoid structures and recurrence of stage II and III colorectal cancer, *Oncoimmunology* 7 (2018), e1378844, <https://doi.org/10.1080/2162402X.2017.1378844>.
- [44] K. Silina, A. Soltermann, F.M. Attar, R. Casanova, Z.M. Uckelely, H. Thut, et al., Germinal centers determine the prognostic relevance of tertiary lymphoid structures and are impaired by corticosteroids in lung squamous cell carcinoma, *Cancer Res.* 78 (2018) 1308–1320, <https://doi.org/10.1158/0008-5472.CAN-17-1987>.
- [45] H.H. Workel, J.M. Lubbers, R. Arnold, T.M. Prins, P. van der Vlies, K. de Lange, et al., A transcriptionally distinct CXCL13(+)/CD103(+)/CD8(+) T-cell population is associated with B-cell recruitment and neoantigen load in human cancer, *Cancer Immunol. Res.* 7 (2019) 784–796, <https://doi.org/10.1158/2326-6066.CIR-18-0517>.
- [46] A.B. Rodriguez, J.D. Peske, V.H. Engelhard, Identification and characterization of tertiary lymphoid structures in murine melanoma, *Methods Mol. Biol.* 1845 (2018) 241–257, https://doi.org/10.1007/978-1-4939-8709-2_14.
- [47] A. Asrir, C. Tardiveau, J. Coudert, R. Laffont, L. Blanchard, E. Bellard, et al., Tumor-associated high endothelial venules mediate lymphocyte entry into tumors and predict response to PD-1 plus CTLA-4 combination immunotherapy, *Cancer Cell* 40 (2022) 318–334 e319, <https://doi.org/10.1016/j.ccell.2022.01.002>.
- [48] H. Kim, C. Rodriguez-Navas, R.K. Kollipara, P. Kapur, I. Pedrosa, J. Brugarolas, et al., Unsaturated fatty acids stimulate tumor growth through stabilization of beta-catenin, *Cell Rep.* 13 (2015) 495–503, <https://doi.org/10.1016/j.celrep.2015.09.010>.
- [49] R. Takada, Y. Satomi, T. Kurata, N. Ueno, S. Norioka, H. Kondoh, et al., Monounsaturated fatty acid modification of Wnt protein: its role in Wnt secretion, *Dev. Cell* 11 (2006) 791–801, <https://doi.org/10.1016/j.devcel.2006.10.003>.
- [50] J. Rios-Esteves, M.D. Resh, Stearoyl CoA desaturase is required to produce active, lipid-modified Wnt proteins, *Cell Rep.* 4 (2013) 1072–1081, <https://doi.org/10.1016/j.celrep.2013.08.027>.